Fabrication and Design of High-Density Carbon Nanostructured Papers with Superior Conductive Properties

Hammad Younes, Rashid Abu Al-Rub, Md. Mahfuzur Rahman, Ahmed Dalaq and Amal Al Ghaferi*
Mechanical and Materials Engineering Department,
Masdar Institute of Science and Technology (MIST)
P.O box 54224, Abu Dhabi, United Arab Emirates.

ABSTRACT

A simple and scalable method are used for the fabrication of high-density Carbon Nanostructured (CNS)-based papers using intrinsically aligned CNS material. As fabricated CNS papers has higher density that has not been reported before, which obtained by applying different pressure load on the BP papers. The SEM study shows a very high degree of alignment due to the intrinsic alignment of CNS, which remained unaltered even after the sonication and the pressing process. With the increase in density, CNS-papers show an improved in the electrical behavior. The electrical conductivity of the papers improves by 113% with increasing the density.

Keywords: carbon nanostructure, alignment, densification, electrical conductivity

1. INTRODUCTION

Carbon nanotubes (CNTs) have attracted significant attention since they were discovered by Lijima in 1991 [1]. Because of their superior properties, CNTs are used in many different applications such as nanocomposites [2] nanofluids [3-7] and grease [8, 9]. Theoretical and experimental studies have shown that single wall nanotubes SWNTs have a tensile modulus of ~ 1 TPa, a tensile strength of~ 50-150 GPa, and a fracture strain of~ 5-10 % [10-13]. CNTs are expected to be very good thermal conductors along the length of the tube. It is shown that multiwall carbon nanotubes (MWNTs) have unusually high thermal conductivity (e.g., 3000 W/mK)[14] which is more than seven times that of copper, a metal well-known for its good thermal conductivity of 385 W/mK [15-17]. Buckypapers have been used since the discovery of CNTs and considerable effort has been conducted on these materials to use them for many different application. Chen et al, reported the fabrication of a binder-free carbon nanomaterials hybrid structure BPs, the BPs were served as conductive scaffold [18]. Chen et al, Studied the effect of CNT structures including CNT diameters and lengths on the formation of the networks of BPs and their thermal conducting performance. [19]. Chen also Prepared buckypapers using well-aligned CNTs arrays. The density of the BP was as high as 1.39 g cm^{-3}. The Young's modulus of the buckypapers could reach a magnitude over 2 GPa. The electrical conductivity changes in the range from 31900−64000 S m^{-1}.[20]

2. MATERIALS AND METHODS

Materials: Sonication was performed using a Sonics Vibra Cell Digital sonicator, model VC 505 (500 watts). The surfactants, sodium dodecylbenzenesulfonate (SDBS) (C18H29NaO3S; MW 348 g/mol) used for the dispersion was obtained from Sigma-Aldrich.

Methods: The CNSs papers were made by dispersing CNSs in di-ionized water, SDDBS was used a surfactant to aid in dispersing CNS. Once the CNS were effectively dispersed in the surfactant solution, they were filtered using Buchner Filtration. The density was computed by the mass and volume of samples, and the thickness of CNT paper was measured by a micrometer.

Characterization Techniques: The microstructures of the samples were probed by scanning electron microscopy (SEM) FEI quanta 250 ESEM and the FEI Nova NanoSEM 650. Atomic force microscopy (AFM) data was obtained using Asylum MFP-3D tool. The parameters were deflection 1.5v, scan speed 0.7 Hz and applied voltage 500v; and contact mode imaging was used. Electrical conductivity was obtained using Lake Shore Hall Effect Measurement (HMS) systems, model 7700A.

3. RESULT AND DISCUSSION

The agglomeration of the tubes with the formation of big bundles is one of the challenges of using CNTs in many applications. Bucky papers have the ability to transfer all the properties that CNTs have into composites. The other challenge is the randomly orientation of the carbon nanotubes embedded in polymers and bulk samples. Alignment of the CNTs parallel to the load direction can highly improve the mechanical, electrical and thermal conductivity of nanocomposites or Bucky papers. This improvement on the electrical and thermal conductivity can be attributed to the anisotropic nature of the nanotubes.[24]. In addition, the aligned CNTs make connected paths through the whole material that enhance conducting heat and electricity. Figure 1 (a) is a camera image of a typical round (diameter 7 cm) aligned CNS paper as prepared by the vacuumed filtration method. The surface of the CNS paper is very smooth as it can be seen in the image. Figure 1 (b) shows a strip made from CNS papers subjected to 100 MPa pressure. The strip look smother and denser.

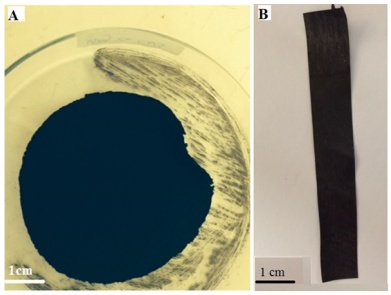

Figure 1 Camera image for (A) a round (diameter 7 cm) aligned CNS paper and (B) strip of CNS papers.

3.1. Densification of Carbon Nanostructure Bps Through Pressing the SEM and Morphology

In order to study the effect of the density of the CNS papers on the electrical and conductivity, CNS papers were prepared and 70-100 MPa pressures have been applied to the BPs. By pressing with different pressures, a BP with density that has not been achieved before and very close to the ultimate density (1.7-1.9 g/cm^3) of BP has been obtained. The density was computed by the mass and volume of samples, and the thickness of CNS paper was measured by a micrometer. The morphology of CNSs and CNSs papers were studied using scanning electron microscopy and atomic force microscopy. SEM and AFM are powerful tools to observe and study the surface of the materials with very high magnifications.

3.1.1. SEM Images For Carbon Nanostructures

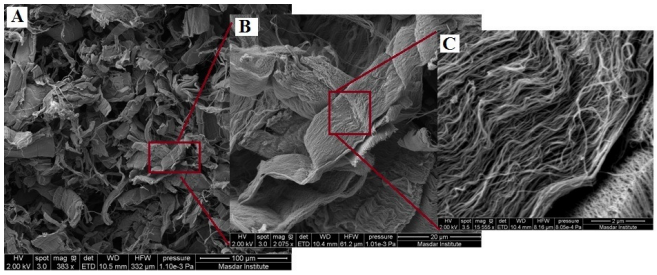

Figure 2 SEM images of the carbon nanostructures (CNS): (a) SEM images shows CNS flacks (b) & (c) SEM zoom showing closely packed and aligned carbon nanotubes (CNTs) within one flack.

image 2 (A) shows that CNSs are flakes made from a huge number of CNTs attached to each other with strong very Van der Waals forces. Image 2 (B & C) are a closer SEM zoom showing clearly that these groups of carbon nanotubes are all aligned in one direction at the same flack or structure.

3.1.2. SEM images for carbon nanostructures papers cross section

Figure 3 shows a cross section SEM images for of the CNS papers. Image (a) at 3µm scale bar and (b) at 100nm scale bar. It can be seen clearly in fig 4 A, that CNS are oriented in one direction. This image shows that using the high-ultrasonication did not break the alignment for the CNS. Image 4 B is a higher magnification image of fig 4 A, which confirms that the CNS are well aligned in the paper and the density is much higher than that of CNS flakes.

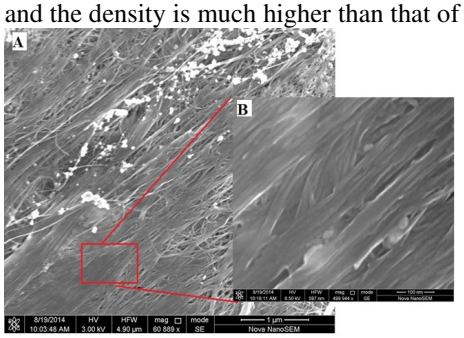

Figure 3 Cross section SEM images for carbon nanostructures papers. Image (a) Cross section SEM image showing the alignment and the closely packed CNS and (b) a closer SEM zoom showing closely packed and aligned carbon nanotubes.

3.1.3. SEM Images For Carbon Nanostructures Papers After Compression

CNSs papers were subjected to a compression at different load in order to reduce the thickness of the papers and thus increase the density.

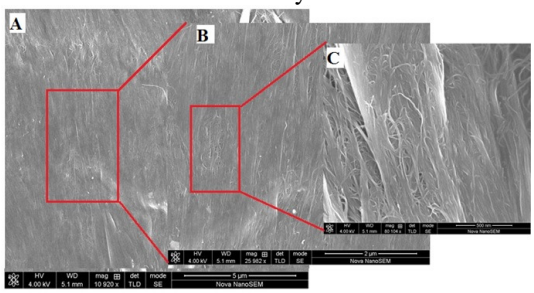

Figure 4 Cross sectional SEM images for compressed carbon nanostructures papers, Image (a) shows the alignment and the closely packed CNS, (b) & (c) SEM zoom showing closely packed and aligned carbon nanotubes

Figure 4 is cross section SEM images for the CNS papers after applying 100 MPa pressure for 10 minutes. CNSs maintain good alignment even after the compression, high packing density CNS papers obtained which will lead to more contact area between the nanotubes.

3.2.AFM Results

Atomic force microscopy CAFM (conductive atomic force microscopy) and d-AFM (non-contact mode) tests were performed to realize the nanoscopic properties of the CNS-papers. Nanoscale alignment of the CNS was realized from the AFM topography obtained by dynamic AFM mode (Figure 5). High electrical conductivity of the paper are discussed by the current map obtained from CAFM spectroscopy scans.

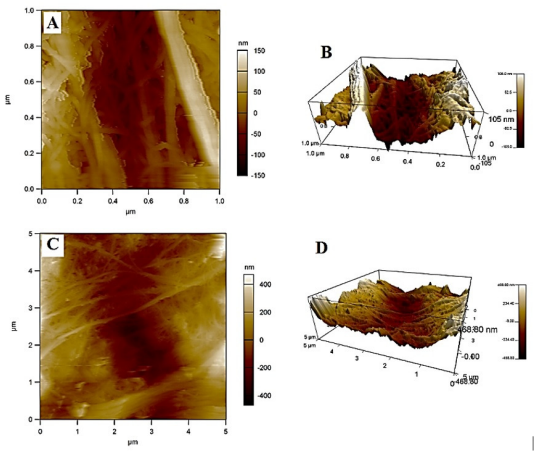

Figure 5 Non-contact mode AFM scans and their corresponding 3D surfaces showing the nanoscale alignment of the CNS in the papers. A &C are the height distribution of two different samples, and B & D are their corresponding 3D images

Figure 5 shows that the directional orientation of the CNs are the key factor in discerning high electrical conductivity as these alignment acts as electrical conduction channel for the transport along the orientation direction.

3.3.Electrical Conductivity

The CNS Ps were prepared with different density and the effect of the density on the electrical resistivity was studied. Figure 6 shows the density of the prepared CNS papers and their electrical conductivity. The densifications of the CNS papers were done by compressing the CNS papers with 50K and 70K N for 10 min. the compression decreases the thickness for each sample and hence decreases the volume and density. The electrical conductivity that obtained at 0.6 gm/cm3 is found to be higher than many of reported data in literature at the same weight density. Díez-Pascual et al, prepared BPs with density equals 0.6 gm/cm3 the electrical conductivity found to be 9–45 S/cm [27]. In other work for the same researcher, the electrical conductivity found to be in the range 47-53 S/cm at temperature 270-375 K [28]. Sakurai et al, found that the electrical conductivity of buckypaper fabricated from SWCNT forest with the heights of 1,500, 700, and 350 µm, respectively is in the range of (19 to 45 S/cm), at density close to 0.6 gm/cm3 [29]. Wang et al, reported the measured electrical conductivity of the 0.6 gm cm^{-1} parallel aligned buckypaper sample to be 2.0 × 102 S cm^{-1} at room temperature. [30]

CNS papers with the higher density exhibit the highest electrical conductivity as seen in Figure 6. By increasing the density by almost two times from 0.64 to 1.23 gm/cm^3, the electrical conductivity improved by 103%, and by increasing the density up to (1.68) the conductivity increased by 111%. In order to understand this behavior and interpret these interesting results, the mechanism of electrical conduction within a CNS papers has to be considered. Figure 2 A shows that there are many flakes made up from CNTs each flake has a groups of CNTs aligned in one direction and all connected to one base. Dispersing these flakes in water by using ultra-high sonicator did not break the alignment of the CNTs inside each groups. Figures 4 shows that there is still an alignment for the CNS even after making the CNSs papers. The CNS P is a 3D network of dispersed CNS, and the electrical conduction occurs either (1) tube–tube within the structure, (2) CNS–CNS within bundle or (3) between neighbor bundles through their contacts. Therefore, the electrical conductivity (σ) depends on the conductivity of the nanotubes themselves and the ability of the electric carriers to tunnel between adjacent nanotubes or adjacent bundles.

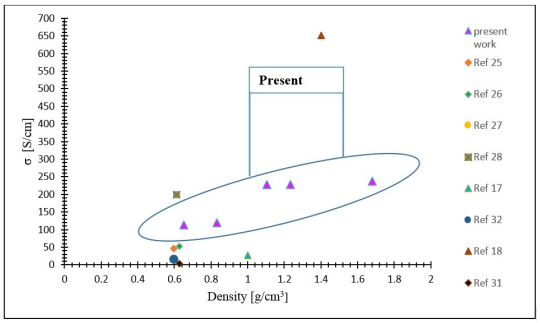

Figure 6 Electrical conductivity of the nanocomposites as a function of density.

3.3.1. Effect of Pressing And Alignment on the Electrical Conductivity

Pressing the CNS Ps increases network density by decreasing the gap within and between CNS creates better contacts and reduce at the same time the electrical resistance by reducing air gaps and providing more conductive pathways for the charge carriers, which yields to an increase in conduction within the CNS papers [30]. We believe that if the surfactant has been removed successfully from the CNS papers the conductivity will be higher, because surfactant blocks the intertube connections and increases intertube contact resistance [31]. In addition, the thickness of the BP will be reduced after washing out all the surfactant, which will increase the density and hence increases electrical conductivity, We fund that the electrical conductivity of our fabricated CNS papers are higher than many of reported data in literature [17-18, 25-28, 31-32]. The alignment of the CNTs inside each nanostructure improves the electrical conductivity of the CNS papers. Aligned CNSs act as conductive channels for the ballistic electron transport. In the randomly aligned nanostructure, the entangled nanotube that ultimately causes an increase in the effective resistance interrupts electron transports. In the conductive AFM Figure 5, the conductive channels are clearly visualized by the current mapping. Alignment reduces the collective effect of steric hindrance (resistance in the electron transport) caused by the entangled nanotubes.

CONCLUSION

High-density CNS-based papers have been fabricated successfully using an anionic surfactant. The electrical conductivity of the CNS papers have been tested. As fabricated CNS papers have higher density than anything reported before and very close to the ultimate density of BP. This is achieved by applying different pressure load on the BP papers. The surface and cross sectional SEM study shows a very high degree of alignment due to the intrinsic alignment of CNS, which remained unaltered during sonication and the pressing process. With the increase in density, CNS-papers showed an improved electrical behavior. The directional orientation of the CNSs are the key factor in discerning high electrical conductivity as these alignment acts as electrical conduction channel for the transport along the orientation direction. The electrical conductivity of the papers improved by 113% with increasing the density. The potential of self-aligned and closely packed CNS with superior electrical conductivity may lead to unprecedented and simultaneous enhancements in the macroscopic electrical, thermal, and mechanical properties made of these self-aligned CNS.

REFERENCE

[1] S. Iijima, nature 354 (6348), 56-58 (1991).
[2] D. W. Abueidda, A. S. Dalaq, R. K. Abu Al-Rub and H. A. Younes, International Journal of Mechanical Sciences 92 (0), 80-89 (2015).
[3] H. Younes, G. Christensen, H. Hong and G. Peterson, Journal of Nanofluids 2 (1), 4-10 (2013).
[4] H. Younes, G. Christensen, M. Liu, H. Hong, Q. Yang and Z. Lin, Journal of Nanofluids 3 (1), 33-37 (2014).
[5] G. Christensen, H. Younes, H. Hong and G. Peterson, Journal of Nanofluids 2 (1), 25-28 (2013).
[6] S. Neupane, S. Khatiwada, C. Jaye, D. A. Fischer, H. Younes, H. Hong, S. P. Karna, S. G. Hirsch and D. Seifu, ECS Journal of Solid State Science and Technology 3 (8), M39-M44 (2014).
[7] H. Younes, G. Christensen, D. Li, H. Hong and A. A. Ghaferi, Journal of Nanofluids 4 (2), 107-132 (2015).
[8] L. Hongtao, J. Hongmin, H. Haiping and H. Younes, Industrial Lubrication and Tribology 66 (5), 579-583 (2014).
[9] H. Hong, D. Thomas, A. Waynick, W. Yu, P. Smith and W. Roy, Journal of Nanoparticle Research 12 (2), 529-535 (2010).
[10] H. Kuzmany, A. Kukovecz, F. Simon, M. Holzweber, C. Kramberger and T. Pichler, Synthetic Metals 141 (1), 113-122 (2004).
[11] S. Cui, R. Canet, A. Derre, M. Couzi and P. Delhaes, Carbon 41 (4), 797-809 (2003).
[12] K. Yurekli, C. A. Mitchell and R. Krishnamoorti, Journal of the American Chemical Society 126 (32), 9902-9903 (2004).
[13] L. Liu, A. H. Barber, S. Nuriel and H. D. Wagner, Advanced Functional Materials 15 (6), 975-980 (2005).
[14] M. Biercuk, M. C. Llaguno, M. Radosavljevic, J. Hyun, A. T. Johnson and J. E. Fischer, Applied physics letters 80 (15), 2767-2769 (2002).
[15] C.-W. Nan, G. Liu, Y. Lin and M. Li, Applied Physics Letters 85 (16), 3549-3551 (2004).
[16] S. Berber, Y.-K. Kwon and D. Tomanek, Physical review letters 84 (20), 4613 (2000).
[17] Z. Spitalsky, D. Tasis, K. Papagelis and C. Galiotis, Progress in polymer science 35 (3), 357-401 (2010).
[18] H. Chen, J. Di, Y. Jin, M. Chen, J. Tian and Q. Li, Journal of Power Sources 237, 325-331 (2013).
[19] H. Chen, M. Chen, J. Di, G. Xu, H. Li and Q. Li, The Journal of Physical Chemistry C 116 (6), 3903-3909 (2012).
[20] L. Zhang, G. Zhang, C. Liu and S. Fan, Nano letters 12 (9), 4848-4852 (2012).
[21] J. Hone, M. Llaguno, N. Nemes, A. Johnson, J. Fischer, D. Walters, M. Casavant, J. Schmidt and R. Smalley, Applied Physics Letters 77 (5), 666-668 (2000).
[22] H. Garmestani, M. S. Al-Haik, K. Dahmen, R. Tannenbaum, D. Li, S. S. Sablin and M. Y. Hussaini, Advanced Materials 15 (22), 1918-1921 (2003).
[23] M. A. Correa-Duarte, M. Grzelczak, V. Salgueirino-Maceira, M. Giersig, L. M. Liz-Marzan, M. Farle, K. Sierazdki and R. Diaz, The Journal of Physical Chemistry B 109 (41), 19060-19063 (2005).
[24] E. Camponeschi, B. Florkowski, R. Vance, G. Garrett, H. Garmestani and R. Tannenbaum, Langmuir 22 (4), 1858-1862 (2006).
[25] M. S. Dresselhaus, G. Dresselhaus, R. Saito and A. Jorio, Physics reports 409 (2), 47-99 (2005).
[26] T. Uchida, M. Tazawa, H. Sakai, A. Yamazaki and Y. Kobayashi, Applied Surface Science 254 (23), 7591-7595 (2008).
[27] A. M. Díez-Pascual and D. Gascón, ACS applied materials & interfaces 5 (22), 12107-12119 (2013).
[28] A. M. Díez-Pascual, J. Guan, B. Simard and M. A. Gómez-Fatou, Composites Part A: Applied Science and Manufacturing 43 (6), 1007-1015 (2012).
[29] S. Sakurai, F. Kamada, D. N. Futaba, M. Yumura and K. Hata, Nanoscale research letters 8 (1), 1-7 (2013).
[30] D. Wang, P. Song, C. Liu, W. Wu and S. Fan, Nanotechnology 19 (7), 075609 (2008).
[31] J. G. Park, J. Smithyman, C.-Y. Lin, A. Cooke, A. W. Kismarahardja, S. Li, R. Liang, J. S. Brooks, C. Zhang and B. Wang, Journal of Applied Physics 106 (10), 104310 (2009).
[32] K. Yang, J. He, P. Puneet, Z. Su, M. J. Skove, J. Gaillard, T. M. Tritt and A. M. Rao, Journal of Physics: Condensed Matter 22 (33), 334215 (2010).